Supporting Materials

Table S1. Selected Bond Distances (Å) and Angles (°) for $Ru_2(\mu\text{-}O_2CMe)_3(\mu\text{-}DXyl^{2,6}F)Cl(HDXyl^{2,6}F)$·toluene (**1b**·toluene)

Bond distances			
Ru(1)−Ru(2)	2.3326(8)		
Ru(1)−N(1)	2.033(6)	Ru(2)−O(2)	2.029(4)
Ru(2)−N(2)	2.051(5)	Ru(2)−O(4)	2.067(5)
Ru(1)−O(1)	2.036(5)	Ru(2)−O(6)	2.043(5)
Ru(1)−O(3)	2.058(5)	Ru(1)−Cl(1)	2.471(2)
Ru(1)−O(5)	2.030(6)	Ru(2)···N(3)	2.388(5)
Bond angles			
N(1)−Ru(1)−O(1)	91.0(2)	N(2)−Ru(2)−O(6)	91.4(2)
N(1)−Ru(1)−O(3)	178.5(2)	N(1)−Ru(1)−Ru(2)	89.5(2)
N(2)−Ru(2)−O(4)	177.9(2)	O(1)−Ru(1)−Ru(2)	88.7(2)
O(1)−Ru(1)−O(3)	89.3(2)	O(1)−Ru(1)−Cl(1)	91.8(2)
O(5)−Ru(1)−O(1)	174.2(3)	Ru(2)−Ru(1)−Cl(1)	178.13(6)
O(2)−Ru(2)−O(6)	175.5(2)	Ru(1)−Ru(2)···N(3)	168.8(2)

Table S2. Selected Bond Distances (Å) and Angles (°) for *trans*-$Ru_2(O_2CMe)_2(DXyl^{2,6}F)_2Cl$·2toluene (**2b**·2toluene)

Bond distances			
Ru(1)−Ru(2)	2.3157(3)	Ru(2)−N(2)	2.047(2)
Ru(1)−N(1)	2.078(2)	Ru(2)−N(4)	2.051(2)
Ru(1)−N(3)	2.079(2)	Ru(2)−O(2)	2.023(2)
Ru(1)−O(1)	2.045(2)	Ru(2)−O(4)	2.024(2)
Ru(1)−O(3)	2.058(2)	Ru(1)−Cl(1)	2.4006(7)
Bond angles			
N(1)−Ru(1)−N(3)	178.32(9)	N(2)−Ru(2)−O(4)	179.76(9)
N(1)−Ru(1)−O(1)	88.39(9)	N(1)−Ru(1)−Ru(2)	89.30(6)
N(3)−Ru(1)−O(1)	91.73(9)	O(1)−Ru(1)−Ru(2)	87.97(6)
O(1)−Ru(1)−O(3)	175.73(8)	O(1)−Ru(1)−Cl(1)	93.05(6)
N(2)−Ru(2)−N(4)	178.65(9)	O(3)−Ru(1)−Cl(1)	91.22(6)
N(2)−Ru(2)−O(2)	89.89(9)	Ru(2)−Ru(1)−Cl(1)	178.94(2)

Table S3. Selected Bond Distances (Å) and Angles (°) for $Ru_2(DAniF)_4Cl{\cdot}0.5CH_2Cl_2$ (**5**$\cdot 0.5CH_2Cl_2$)

Bond distances			
Ru(1)−Ru(2)	2.3960(4)	Ru(2)−N(2)	2.048(1)
Ru(1)−N(1)	2.074(2)	Ru(1)−Cl(1)	2.4380(8)
Bond angles			
N(1)−Ru(1)−N(1A)	175.59(7)	N(1)−Ru(1)−Ru(2)	87.79(4)
N(1)−Ru(1)−N(1B)	89.916(6)	N(1)−Ru(1)−Cl(1)	92.21(4)
N(2)−Ru(2)−N(2A)	179.45(7)	Ru(2)−Ru(1)−Cl(1)	180.0
Torsion angle			
N(1)−Ru(1)−Ru(2)−N(2)	7.4(4)		

Table S4. Selected Bond Distances (Å) and Angles (°) for [*trans*-$Ru_2(\mu\text{-}OMe)_2(\mu\text{-}O_2CMe)_2(HDAniF)_4]Cl_2\cdot 4MeOH$ (**6**·4MeOH)

Bond distances			
Ru(1)−Ru(1A)	2.5009(7)		
Ru(1)−N(1)	2.065(4)	Ru(1)−O(6)	2.083(3)
Ru(1)−N(3)	2.080(4)	Ru(1)−O(7)	2.022(3)
Ru(1)−O(5)	2.083(3)	Ru(1A)−O(7)	2.023(3)
Bond angles			
O(5)−Ru(1)−O(6)	173.4(1)	N(1)−Ru(1)−O(5)	92.3(1)
N(1)−Ru(1)−O(7)	170.3(2)	O(7)−Ru(1)−O(7A)	103.6(1)
N(1)−Ru(1)−N(3)	85.5(2)	O(6)−Ru(1)−Ru(1A)	86.9(1)
N(1)−Ru(1)−O(6)	92.3(1)	Ru(1)−O(7)−Ru(1A)	76.4(1)

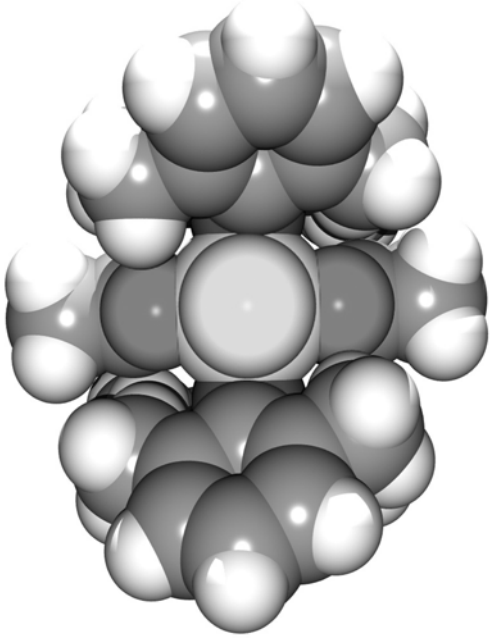

Figure S1. Space-filling model of *trans*-$Ru_2(O_2CMe)_2(DXyl^{2,6}F)_2Cl(THF)$ (**2a)** as viewed along the Cl−Ru−Ru axis.

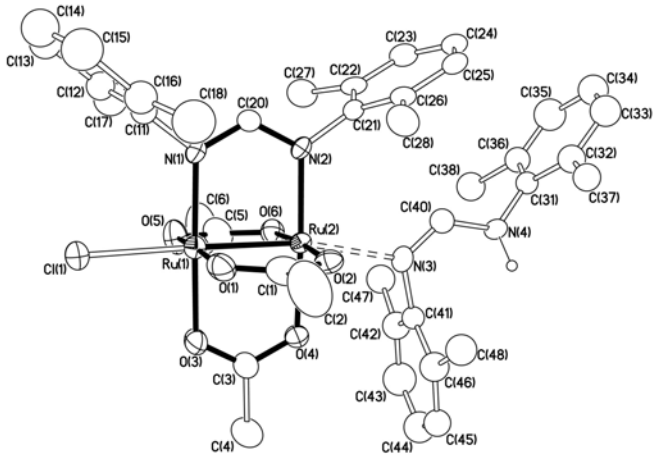

Figure S2. A view of $Ru_2(O_2CMe)_3(DXyl^{2,6}F)Cl(THF)(HDXyl^{2,6}F)$ in **1b**·toluene with atoms represented by thermal ellipsoids at the 35% probability level. H atoms are omitted for clarity. Selected bond distances (Å) are: Ru(1)–Ru(2) 2.333(1), Ru(1)–N(1) 2.033(6), Ru(2)–N(2) 2.051(5), Ru(1)–Cl(1) 2.471(2), and Ru(2)···N(3) 2.388(5).

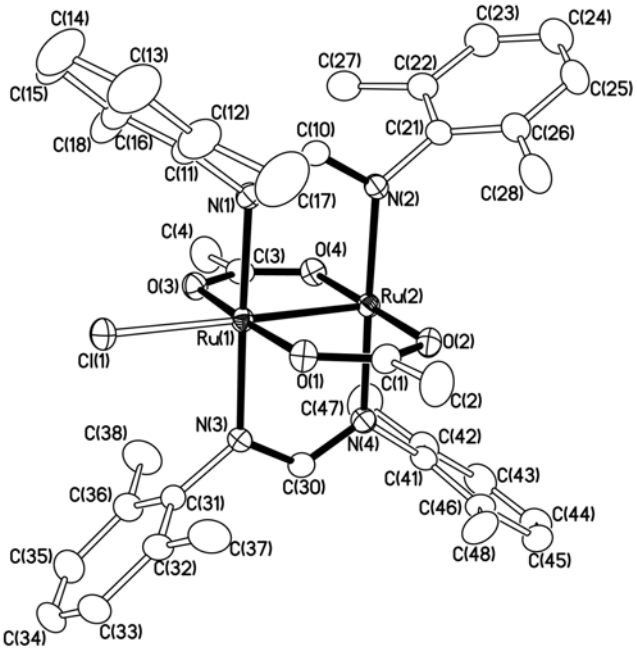

Figure S3. A view of *trans*-$Ru_2(O_2CMe)_2(DXyl^{2,6}F)_2Cl$ in **2b**·2toluene with the atoms represented by thermal ellipsoids at the 35% probability level. H atoms are omitted for clarity. Selected bond distances (Å) are: Ru(1)–Ru(2) 2.316(1), Ru(1)–N(1) 2.078(2), Ru(2)–N(2) 2.047(2), and Ru(1)–Cl(1) 2.401(1).

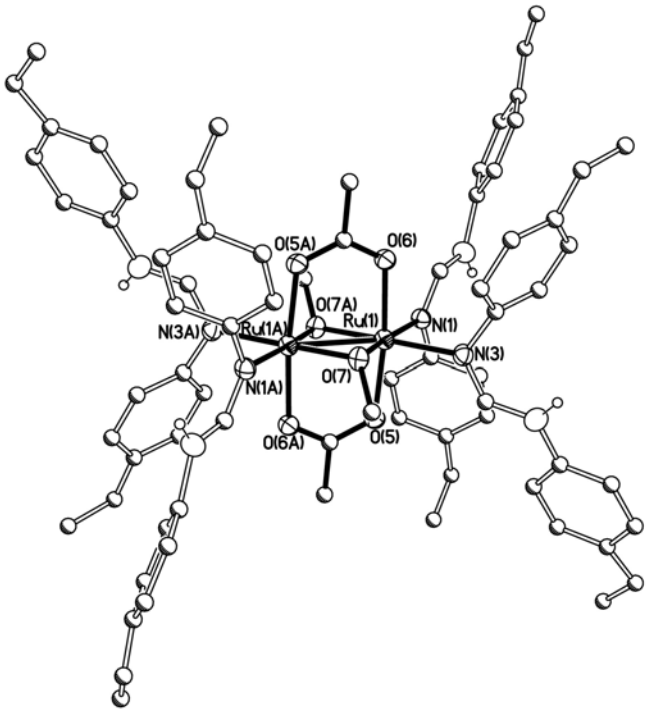

Figure S4. A view of [*trans*-$Ru_2(\mu\text{-}OMe)_2(\mu\text{-}O_2CMe)_2(HDAniF)_4]^{2+}$ in **6**·4MeOH with the atoms represented by thermal ellipsoids at the 35% probability level. C atoms and O atoms of the HDAniF ligands are presented as spheres of arbitrary radii. H atoms, except those of the N atoms of the HDAniF ligands, are omitted for clarity. Selected bond distances (Å) are: Ru(1)–Ru(1A) 2.501(1), Ru(1)–N(1) 2.065(4), Ru(1)–N(3) 2.079(4), Ru(1)–O(5) 2.084(3), Ru(1)–O(6) 2.082(2), Ru(1)–O(7) 2.0022(3), and Ru(1A)–O(7) 2.021(3).

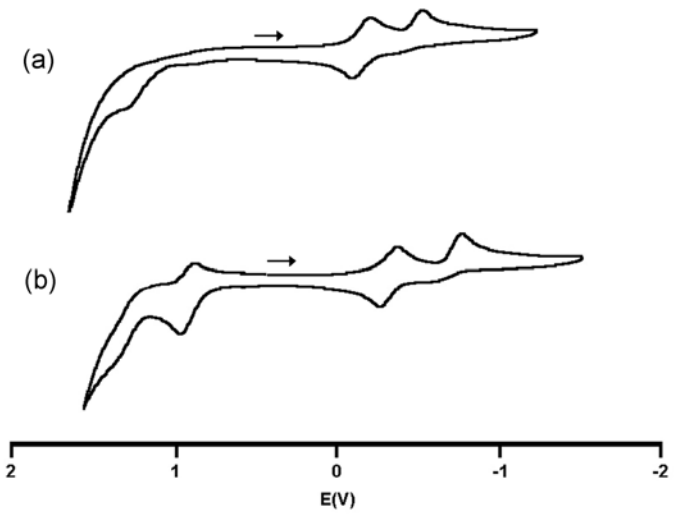

Figure S5. Cyclic voltammograms of **1a** (a) and **2a** (b).

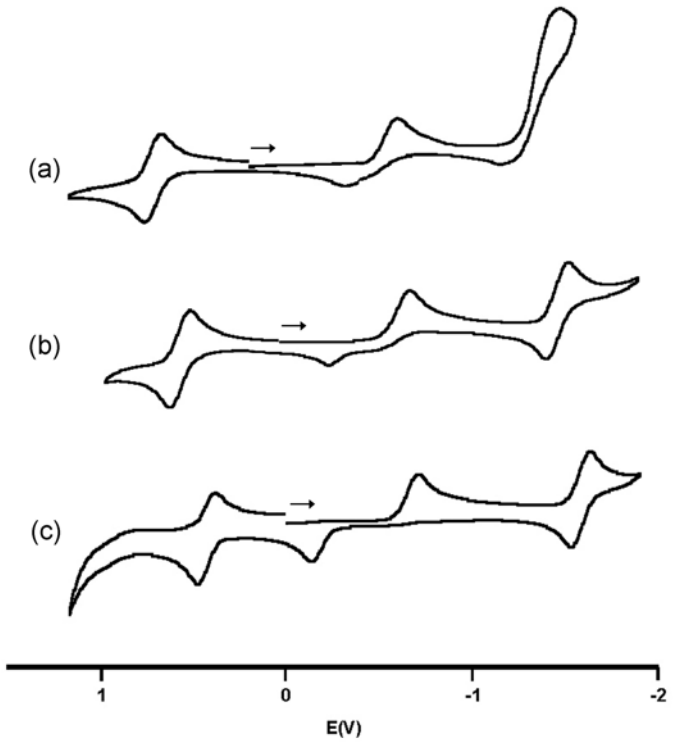

Figure S6. Cyclic voltammograms of *cis*-$Ru_2(O_2CMe)_2(DAniF)_2Cl$ (a), $Ru_2(O_2CMe)(DAniF)_3Cl$ (b), and **5** (c).